

## FRONT SIDE IMPROVEMENTS FOR N-PASHA SOLAR CELLS

G.J.M. Janssen<sup>1\*</sup>, M. Koppes<sup>1</sup>, Y. Komatsu<sup>1</sup>, J. Anker<sup>1</sup>, J. Liu<sup>1</sup>, A. Gutjahr<sup>1</sup>, A.A. Mewe<sup>1</sup>,  
C.J.J. Tool<sup>1</sup>, I.G. Romijn<sup>1</sup>, O. Siarheyeva<sup>2</sup>, M. Ernst<sup>2</sup>, B.W.H. van de Loo<sup>3</sup>, W.M.M. Kessels<sup>3</sup>

<sup>1</sup>ECN Solar Energy, P.O. Box 1, NL-1755 ZG Petten, The Netherlands

<sup>2</sup>Levitech BV, Versterkerstraat 10, NL-1322 AP Almere, The Netherlands

<sup>3</sup>Eindhoven University of Technology, Department of Applied Physics, P.O. Box 513,  
NL-5600 MB Eindhoven, The Netherlands

\*Email: [ianssen@ecn.nl](mailto:ianssen@ecn.nl); Phone: +31 88 515 4803; Fax: +31 88 515 8214

**ABSTRACT:** We present a new approach to improve the efficiency of n-type solar cells by tuning the boron emitter doping profile and optimizing the surface passivation. The boron emitter profile is tuned using a new method of just etching the surface by 10-30 nm. The etching was carried out after diffusion and glass removal. This resulted in a boron emitter without boron depletion at the surface, a higher  $V_{OC}$  by 6 mV and a higher efficiency by 0.2% absolute. To improve the surface passivation, we found that a very high implied  $V_{OC}$  of  $680 \pm 2$  mV can be obtained with an improved pre-cleaning followed by a wet chemical surface oxidation and ALD  $Al_2O_3$  capped with PECVD-SiN<sub>x</sub>.

**Keywords:** n-type, boron, passivation, performance

### 1 INTRODUCTION

ECN works with partners on the improvement of the efficiency of bifacial n-Pasha solar cells and modules using cost effective and industrial processing. In recent years, improvements of Back Surface Field (BSF) and metallization resulted in a highest efficiency of 20.4%, and average efficiencies of 20.2% [1]. In the present work, the focus shifts to the emitter and its passivation. The purpose of the work presented in this paper is to show cost effective and industrial solutions for the tuning of boron emitters, surface preparation and passivation.

A previously published loss analysis identified the boron emitter and its passivation as one of the current limiting factors for high efficient n-type front junction solar cells [2]. In that study it was found that the surface recombination rate accounts for about 50% of the total recombination rate associated with the passivated emitter, the balance being Auger recombination. Whereas the Auger recombination rate is related to high doping concentrations and therefore has a trade-off in the form of a low sheet resistance and an ensuing better fill factor, the surface recombination merely reduces both  $V_{OC}$  and  $J_{SC}$ . Minimization of surface recombination is therefore a prerequisite for a high cell efficiency.

The surface recombination rate is determined by the defect density at the surface ( $D_{it}$ ) and the concentration of minority charge carriers at the surface, and therefore a reduction of either, or both, will lead to improved cell efficiency. This has been the rationale behind all commonly used passivation schemes that rely on chemical passivation to reduce the  $D_{it}$ , or on heavy doping or on built-in surface charges of the passivation layer to reduce the minority carrier concentration [3]. In this study we also considered etching of the boron depletion layer as a means to reduce the minority surface concentration. Such an etching is not expected to result in a large increase of the sheet resistance.

Experimentally the  $D_{it}$  and the minority carrier concentration are not well accessible. To further explain and distinguish the role of the  $D_{it}$  and the minority carrier surface concentration, the experimental work was complemented by numerical simulations.

### 2 EXPERIMENTAL

#### 2.1 Etched boron profiles

Boron profiles using the standard ECN  $BBr_3$  diffusion process were applied on textured n-type Cz wafers. This typically results in emitters with a 60 ohm/sq sheet resistance. A wet-chemical etch was then applied to remove 10-30 nm of this emitter. The emitter was further passivated by application of our patented technology of chemical oxidation [4] and PECVD application of a 70 nm thick SiN<sub>x</sub> layer. Symmetrical test structures featuring identical emitters at both sides of the wafer as well as complete n-Pasha cells [1] containing this emitter were made. The resulting boron profiles were measured by Electrochemical Capacitance-Voltage (ECV), as described previously [5]. Quasi-Steady-State Photo Conductance (QSS-PC) was used to measure the implied  $V_{OC}$  of the test structures. Finally of complete n-Pasha cells including the modified emitter were made and the  $IV$  characteristics measured.

#### 2.2 Modified surface passivation

Standard, unetched  $BBr_3$  diffusion profiles were made on one side of a textured n-type Cz wafer. Modifications of the subsequent steps were considered:

- changing the chemical pre-treatment (originally a diluted HF dip)
- application of an ALD  $Al_2O_3$  layer using a Levitrac tool developed by Levitech [6]. This layer has a thickness of about 2 nm.

The passivation was completed by applying a PECVD SiN<sub>x</sub> capping layer. In these experiments no symmetrical test samples were made but implied  $V_{OC}$  measurements were done on structures that included the BSF but did not have any metallization. After metallization the  $IV$  characteristics of the cells were measured.

### 3 NUMERICAL SIMULATIONS

The semi-conductor device modelling package Atlas from Silvaco was used [7] to calculate  $J_{0E}$ , the recombination current prefactor or dark saturation current density of the emitter. The procedure was as described in a previous paper [2]. It is of importance to notice that 1)

the Klaassen parametrization of the band gap is used, 2) the effect of texture is included by scaling the Auger recombination and the surface recombination by a factor 1.7, 3) resulting  $J_{OE}$  values are reported with an intrinsic carrier concentration  $n_i$  of  $8.6 \cdot 10^9 \text{ cm}^{-3}$ , corresponding to  $T=298 \text{ K}$ , the temperature at which the implied  $V_{OC}$  measurements were done.

The recombination prefactor can be related to the implied  $V_{OC}$  of the symmetrical test structures with unetched emitter by:

$$V_{oc,impl} = \frac{kT}{q} \ln \left( \frac{J_L}{2J_{OE} + J_{0,bulk}} + 1 \right) \quad (1)$$

Here  $J_L$  is the generated current and  $J_{0,bulk}$  represents the bulk recombination. Note that both parameters are not well accessible by experiment but may be considered to be the same for the test structures that just differ in etch depth.

In the case of the test structures used for the emitters with modified surface passivation the relation becomes:

$$V_{oc,impl} = \frac{kT}{q} \ln \left( \frac{J_L}{J_{OE} + J_{0BSF} + J_{0,bulk}} + 1 \right) \quad (2)$$

It assumed that  $J_{0BSF}$ , the contribution of the BSF, is the same for all structures.

## 4 RESULTS AND DISCUSSION

### 4.1 Etched boron emitter profiles

Standard diffused 60 ohm/sq boron emitters exhibit a boron-depleted region in the first 10 – 30 nm of the profile. A typical boron emitter profile is shown in the blue line in Figure 1a, as profile 1.

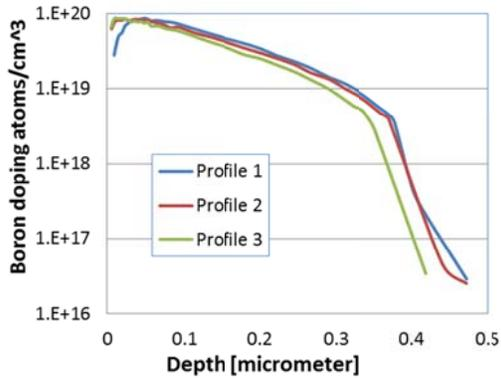


**Figure 1:** ECV profiles of the three different boron profiles as measured with ECV

The standard profile (profile 1) exhibits a boron-depleted region within the first 10 to 30 nm. The depleted region originates from the higher solubility of boron in  $\text{SiO}_2$  than in Si.  $\text{SiO}_2$  is intentionally formed after boron diffusion to reliably remove the boron-rich layer (BRL), a Si-B compound which is otherwise difficult to remove and is detrimental to surface passivation [8]. In our current experiments, we etch this boron-depleted region by 10-30 nm with negligible damage to the surface texture. The wet-chemical oxide passivation process [4] does not re-introduce boron depletion due to its low

process temperature. The resulting boron emitter profile then corresponds to profile 2 or 3 in Figure 1a, depending on the etch depth. Profile 1 and 2 both result in  $R_{sheet}$  of 60 ohm/sq, profile 3 has a  $R_{sheet}$  of 85 ohm/sq.

Figure 2 shows the implied  $V_{OC}$  data obtained with symmetrically diffused lifetime samples with emitter profiles 1, 2 and 3. Etching of the profile results in a gain of 12 mV in implied  $V_{OC}$ . This corresponds to a  $J_0$  improvement of the sample by  $100 \text{ fA/cm}^2$ , i.e.  $50 \text{ fA/cm}^2$  for  $J_{OE}$  on each side.

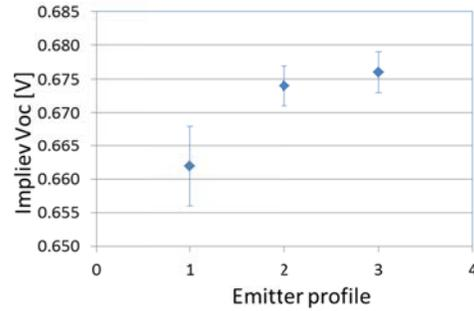


**Figure 2:** Implied  $V_{OC}$  for the symmetrically diffused lifetime samples with emitter profiles 1, 2 and 3 from Figure 1

Numerical simulations can shed further light on the origin of this improvement. Figure 3 shows the calculated  $J_{OE}$  as a function of the surface recombination velocity SRV. In the context of a p+ emitter SRV is the effective electron recombination parameter  $S_{n,eff}$ , which is determined by the interface defect density  $D_{it}$  and the density of fixed charges at the interface  $Q_f$  [9].

According to Figure 3 the  $J_{OE}$  values of the emitter profiles are very sensitive to this parameter. It is also clear that in the range of SRV values  $< 1 \cdot 10^5 \text{ cm/s}$ , relevant for passivated surfaces, the etched profiles (2 & 3) have lower  $J_{OE}$  than the unetched profile (1).

The limit of  $J_{OE}$  at low SRV represents the Auger contribution. Profile 1 & 2 have the same Auger contribution, but at intermediate SRV (around  $1 \cdot 10^4 \text{ cm/s}$ ) the  $J_{OE}$  value of profile 2 is  $20 \text{ fA/cm}^2$  lower than that of the unetched profile. The difference between profile 1 & 3, which has a slightly lower Auger recombination but also a higher  $R_{sheet}$  value, is even more profound,  $40 \text{ fA/cm}^2$ . It must be noted that this trend is opposite to what is usually calculated for deeply etched profiles or lightly doped profiles where a decreasing Auger limit corresponds to an increased sensitivity of  $J_{OE}$  to SRV. This is due to the superficial etching used here that removes the depletion layer but leaves the heavily doped region intact, and therefore the shielding capacity.

The reduction in  $J_{OE}$  that was estimated from the implied  $V_{OC}$  data is larger than can be explained on basis of the etching alone. This result strongly suggests that removing the surface depletion region reduces the surface recombination not only through reduction of the minority carrier concentration, but also through reduction of the SRV, i.e. the  $D_{it}$  or the  $Q_f$ . In this case we estimate the reduction to be in from  $\text{SRV}=15000$  to  $5000 \text{ cm/s}$ , as indicated in Figure 3. This also implies that in our samples the SRV at the boron diffused surfaces does not seem to increase with the boron concentration. This is opposite to what has been reported in the literature for phosphorous n+ type emitters [10]. The results suggest

that the etching may improve chemical passivation or lead to a change in fixed charges, i.e. less positive or more negative  $Q_f$  values. Note, however, that effect of fixed charges at high doping levels is limited, as recently shown by Black et al. [9]. In the samples studied by Black the  $D_{it}$  was found to be independent of the boron concentration in the range between  $1 \cdot 10^{16}$ - $1 \cdot 10^{20}$   $\text{cm}^{-3}$ . We tentatively suggest that the etching procedure provides a better surface pre-treatment for the subsequent passivation scheme.

In the next section further evidence is presented that shows that the SRV of the boron-NAOS-SiN<sub>x</sub> is very sensitive to surface treatment after removal of the BRL and before the wet-chemical oxidation step.

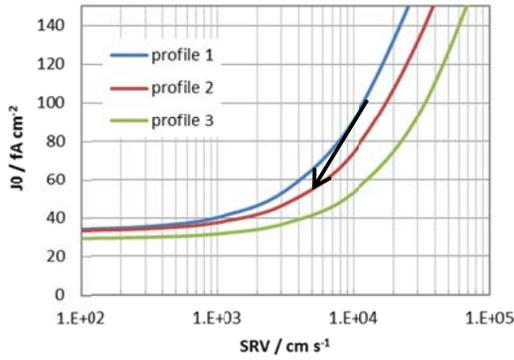


**Figure 3:** Calculated  $J_0$  values for the different boron emitters as function of SRV.

The beneficial effect of reducing the boron depleted region was confirmed by cell results. In this initial test on cell level, only profile 1 and 2 are compared, both with an  $R_{sheet}$  of 60  $\text{ohm/sq}$ . The  $V_{OC}$  increase of  $\sim 6$  mV of n-Pasha cells is in agreement with the  $J_{OE}$  reduction of  $\sim 50$   $\text{fA/cm}^2$ , resulting in an efficiency gain of  $\sim 0.2\%$  absolute, as can be seen in Table I. To enable even higher efficiencies, emitter profile 3 can be appropriate. However, this emitter has a higher sheet resistance, and the front side metallization pitch will need to be adjusted for optimal efficiency.

**Table I:** Averaged (10 cells) IV results for cells with emitters with profiles 1 and 2 (both 60  $\text{ohm/sq}$ )

	$J_{sc}$ ( $\text{mAcm}^{-2}$ )	$V_{oc}$ (V)	FF (-)	$\eta$ (%)
Profile 1	39.0	0.646	0.784	19.7
Profile 2	39.1	0.652	0.779	19.9

#### 4.2 Surface passivation improvements

The possibility to reduce the SRV by surface modification was confirmed by tests in which a different chemical pre-treatment (originally a diluted HF dip) was used before the wet-chemical oxidation step. Table II shows that a modification of the chemical pre-treatment alone already resulted in a gain in cell efficiency of 0.3% absolute. This is mainly due to the increase in  $V_{OC}$  by 6 mV.

**Table II:** Averaged (18 cells) IV results for cells with standard and improved pre-treatment for the wet chemical oxidation step.

	$J_{sc}$ ( $\text{mAcm}^{-2}$ )	$V_{oc}$ (V)	FF (-)	$\eta$ (%)
Standard	39.0	0.649	0.785	19.8
Improved	38.9	0.655	0.788	20.1

In Figure 4a the effect of the improved chemical pre-treatment with and without  $\text{Al}_2\text{O}_3$  on the implied  $V_{OC}$  is shown. The improved pre-treatment and the  $\text{Al}_2\text{O}_3$  both increase the lifetime (shown as implied  $V_{OC}$  in Figure 4a), i.e. reducing  $J_{OE}$ . The lifetime samples were made with an emitter on one side and a BSF on the other. An increase of the implied  $V_{OC}$  from 664 mV towards 676 mV corresponds to a decrease in  $J_{OE}$  by  $\sim 70$   $\text{fA/cm}^2$ , e.g. from  $\sim 110$   $\text{fA/cm}^2$  down to  $\sim 40$   $\text{fA/cm}^2$ . According to the curve for profile 1, this corresponds to a decrease in SRV of an order of magnitude, from 15000  $\text{cm/s}$  to about 1000  $\text{cm/s}$ . At an SRV value of 1000  $\text{cm/s}$  the  $J_{OE}$  of the emitter is close to the limit determined by Auger recombination.

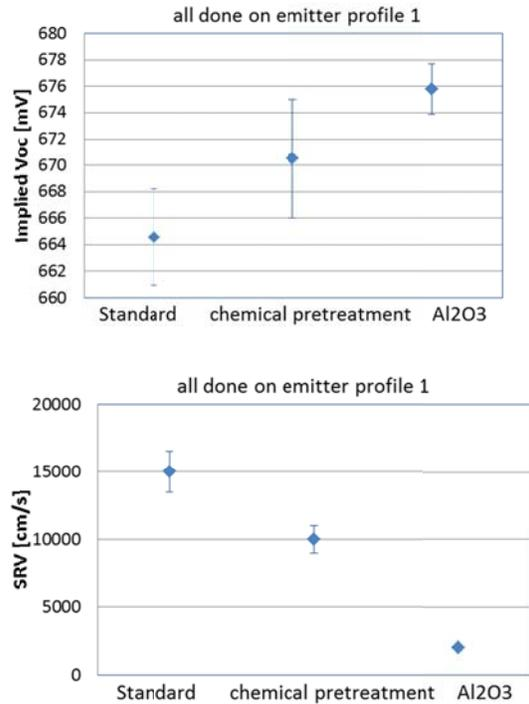


**Figure 4:** Implied  $V_{OC}$  (a) and SRV values (b) for the subsequent improvements for surface passivation

The reduction of the apparent SRV by application of a thin ALD  $\text{Al}_2\text{O}_3$  can have two origins. The first one is that the  $D_{it}$  is reduced, the other is reduction of the minority carriers (electrons) by negative fixed charges that are present at the  $\text{Al}_2\text{O}_3/\text{NAOS}$  interface. For lightly-doped p-type material both mechanisms were found to be effective [11]. Good surface passivation by  $\text{Al}_2\text{O}_3$  for heavily doped p-type silicon has also been reported [12]. But as mentioned in section 4.1, at doping levels in the order of  $10^{20}$   $\text{cm}^{-3}$  the effect of fixed charges is strongly reduced, as was shown in the paper by Black et al. [9]. This suggests that the improved passivation observed in this study may

be mostly due an improved chemical passivation, caused by the presence of an Al<sub>2</sub>O<sub>3</sub> layer between the SiO<sub>2</sub> and SiN<sub>x</sub> layers.

#### 4.3 Implementation at cell level

The current n-Pasha baseline process typically has an average efficiency of >20% and relies on the emitter profile 1 and passivation schemes as in the reference groups in this experiment. Compared to the reference groups the present n-Pasha baseline process includes some rear side improvements. Cell runs on high quality Cz material resulted in 20.4% top efficiencies, as shown in Table III.

**Table III:** IV results for standard n-Pasha ‘baseline’ solar cells (in-house measurements, spectral mismatch corrected)

	Jsc (mA/cm <sup>2</sup> )	Voc (V)	FF (-)	eta (%)
Avg(12cells)	38.9	0.651	0.797	20.2
top	39.2	0.654	0.800	20.4

The improved oxidation pre-treatment and the etching of the boron depletion layer have been implemented on n-MWT cells by ECN. The recent excellent results (up to 20.8% efficiency measured in-house, including spectral mismatch correction) obtained for the n-MWT cells can be partly attributed to these modifications [13].

It must be noted that the efficiency gains related to modified profiles and improved passivation are not always additive. In the case of a very low SRV value, resulting in an  $J_{0E}$  limited by Auger recombination, reduction of the boron depletion layer will not lead to further improvement.

## 4 CONCLUSIONS

Important steps were made to improve the front side passivation of the n-Pasha cell. The high surface recombination can be minimized by either reducing the minority carrier concentration or by reducing the  $D_{it}$ . In all cases the sheet resistance is not affected. One viable option is to remove the boron depletion layer that normally exists in the first 10-30 nm of the profile. The  $J_{0E}$  of the standard 60 ohm/sq emitter improved from 100 fA/cm<sup>2</sup> to 70/55 fA/cm<sup>2</sup> by removing the boron depleted region. The  $J_{0E}$  reduction resulted in a  $V_{OC}$  gain of 6 mV and efficiency gain of 0.2% absolute on cell level.

The most important progress in optimizing the passivation stack is that by improving the pre-cleaning, preceding the wet-chemical oxidation step, and by introducing ALD Al<sub>2</sub>O<sub>3</sub> capped with PECVD-SiN<sub>x</sub> the implied  $V_{OC}$  can be improved by almost 20 mV to 680 mV, realizing a reduction in SRV from >10<sup>4</sup> cm/s to <1000 cm/s. Combining the improved emitter profile and the improved surface passivation values of  $J_{0E}$  close to the Auger limit of 40 – 50 fA/cm<sup>2</sup> are within reach for 60 ohm/sq emitters without compromising on the sheet resistance or the contact resistance.

Implementation of these modifications will result in a large step towards efficiencies of 21% with n-Pasha cells.

## REFERENCES

- [1] I.G. Romijn, B.B. v. Aken, P.C. Barton, A. Gutjahr, Y. Komatsu, M. Koppes, E. Kossen, M.W.P.E. Lamers, D.S. Saynova, C.J.J. Tool, and Y. Zhang, 28th EUPVSEC, Paris (2013).
- [2] G.J.M. Janssen, A. Gutjahr, A.R. Burgers, D.S. Saynova, I. Cesar, and I.G. Romijn, 28th EUPVSEC, Paris (2013).
- [3] A.G. Aberle, *Crystalline Silicon Solar Cells; Advanced Surface Passivation and Analysis*, Center for Photovoltaic Engineering, University of New South Wales, Sydney, Australia, 1999.
- [4] V.D. Mihailetchi, Y. Komatsu, and L.J. Geerligs, Appl.Phys.Lett. 92 (2008) 063510-063513.
- [5] Y. Komatsu, D. Harata, E.W. Schuring, A.H.G. Vlooswijk, S. Katori, S. Fujita, P.R. Venema, and I. Cesar, Energy Procedia 38 (2013) 94-100.
- [6] I. Cesar, E. Granneman, P. Vermont, H. Khatri, A. Shaikh, P. Manshanden, I.G. Romijn, and A.W. Weeber, 38th IEEE Photovoltaic Specialists Conference (2012).
- [7] Atlas, [www.silvaco.com](http://www.silvaco.com), (2013).
- [8] A.H.G. Vlooswijk, P. Venema, and Y. Komatsu, Boron processing in solar cell industry: Boron diffusion in silicon wafers, in *Boron: Compounds, Production and Application*, G.L. Perkins, Ed., p. 543-549, Nova Science Publishers, New York (2010).
- [9] L.E. Black, T. Allen, K.R. McIntosh, and A. Cuevas, J.Appl.Phys. 115 (2014) 093707.
- [10] P.P. Altermatt, J.O. Schumacher, A. Cuevas, M.J. Kerr, S.W. Glunz, R.R. King, G. Heiser, and A. Schenk, J.Appl.Phys. 92 (2002) 3187-3197.
- [11] B. Hoex, J.J.H. Gielis, M.C.M. van de Sanden, and W.M.M. Kessels, J.Appl.Phys. 104 (2008) 113703-113707.
- [12] B. Hoex, J. Schmidt, R. Bock, P.P. Altermatt, M.C.M. van de Sanden, and W.M.M. Kessels, Appl.Phys.Lett. 91 (2007) 112107-3.
- [13] N. Guillevin, L.J. Geerligs, L. Okel, B.B. van Aken, I.J. Bennett, A. Gutjahr, J. Wang, Z. Wang, J. Zhai, Z. Wan, S. Tian, Z. Hu, G. Li, B. Yu, and J. Xiong, 29th EUPVSEC, Amsterdam (2014).